

Ablation of GaAs by Intense, Ultrafast Electronic Excitation from Highly Charged Ions

T. Schenkel, A. V. Hamza, A. V. Barnes, and D. H. Schneider
Lawrence Livermore National Laboratory, Livermore, California 94550

J. C. Banks and B. L. Doyle
Sandia National Laboratory, Albuquerque, New Mexico 87185-1056
(Received 16 March 1998)

We have measured total ablation rates and secondary ion yields from undoped GaAs(100) interacting with slow ($v = 6.6 \times 10^5$ m/s), very highly charged ions. Ablation rates increase strongly as a function of projectile charge. Some 1400 target atoms are removed when a single Th^{70+} ion deposits a potential energy of 152.6 keV within a few femtoseconds into a nanometer-sized target volume. We discuss models for ablation of semiconductors by intense, ultrafast electronic excitation. [S0031-9007(98)07165-8]

PACS numbers: 79.20.Rf, 34.50.Fa

The interaction of slow ($v < 2 \times 10^6$ m/s) highly charged ions (SHCI) with surfaces is an active field of research [1,2] with applications in materials analysis [3] and modification [4–7]. In slow ion-solid collisions, where the projectile velocity is smaller than the Bohr velocity ($v_{\text{Bohr}} = 2.19 \times 10^6$ m/s), most target electrons move faster than the projectile and readily react to the perturbation during a collision. SHCI, such as Xe^{44+} and U^{90+} , are extracted from electron beam ion traps (EBIT) [1] while fast ($v \gg v_{\text{Bohr}}$) highly charged ions are formed by charge state equilibration in gaseous or solid targets using heavy ion accelerators. Charge states of SHCI are far in excess of mean equilibrium charge states formed by slow ions when traveling through solids. The latter are $\sim 1+$ at the velocities selected in this study [8]. Consequently, SHCI neutralize and deexcite rapidly when they interact with solid surfaces. Charge state equilibration times are in the order of a few femtoseconds [8]. The potential energy of SHCI, i.e., the sum of the binding energies of electrons removed to form the ion, is deposited during deexcitation. Individual SHCI deposit tens to hundreds of keV of potential energy into a small (nanometer scale) target volume at the surface. Insulators and thin (~ 10 nm) semimetallic conductors react to this intense, ultrafast, and localized electronic excitation by emission of large numbers of neutral particles [5,9] and secondary ions [3,9]. For bulk semiconductors, no increase of ablation rates as a function of projectile charge was observed for Si interacting with Ar^{q+} , $q \leq 9+$ [10]. Reports for GaAs are controversial. Using Ar^{q+} , $q \leq 9+$, Varga *et al.* [5] found no increase of the sputtering yield with charge. The null result was interpreted in the context of a model of defect-mediated potential sputtering. For the same projectiles, Mochji *et al.* [7] observed a charge dependent sputter yield increase, and the results were interpreted using a Coulomb explosion model [11]. The ionization probability for secondary ions was not determined in either of these two studies. In this Letter we report on measurements of charge state

dependencies of total sputtering and secondary ion yields from GaAs interacting with slow, very highly charged ions up to Th^{70+} . Using projectiles in much higher charge states than were used in earlier studies [5,7,10], we find results that do not follow predictions of established defect mediated or Coulomb explosion models of electronic sputtering. Stimulated by this discrepancy, we discuss structural instabilities [12] induced by intense, ultrafast electronic excitations imposed on GaAs targets in the course of SHCI deexcitation as a microscopic sputtering mechanism.

Highly charged ions were extracted from the electron beam ion trap at Lawrence Livermore National Laboratory [1]. The experimental setup has previously been described [1,3]. Undoped GaAs(100) targets were cleaned *in situ* by repeated cycles of low energy Xe-ion sputtering and annealing at ~ 600 K. Low energy electron diffraction was used to establish a protocol for sputter cleaning and annealing. Surface conditions were monitored by highly charged ion-based time-of-flight secondary ion mass spectrometry (TOF-SIMS) [3]. The pressure in the target chamber was kept below 10^{-9} torr. Samples were cleaned and annealed before each exposure with SHCI. Exposures were not performed in the order of increasing projectile charge states on a given sample. A possible effect of defect accumulation in the sample on sputter yields [13] can thus be excluded. We used the catcher target technique for measurements of total ablation rates [14]. SHCI impinged on GaAs targets with an incident angle of 30° . Silicon dioxide catchers were placed in parallel to the sputter target at a distance of 6 mm, and secondary neutrals and ions emitted from the target during exposure to SHCI were collected on the catcher. SHCI fluxes ranged from $\sim 10^5$ Th^{70+}/s to 3.5×10^6 Xe^{27+}/s . Accurate flux determination is crucial for our experiment. The flux was determined by single ion pulse counting of projectiles impinging on a microchannel plate detector (MCP). Bias voltages and discrimination levels in counting electronics were carefully set to assure constant

detection efficiencies for ions of all charge states and impact energies. The MCP used for direct detection of SHCIs was calibrated by single ion counting in a Daly detector arrangement [15]. The strong burst of secondary electrons emitted by individual SHCIs ($q \geq 27$) incident on solid targets allows for their detection with 100% efficiency [3]. The efficiency of the MCP for direct detection of SHCIs at the bias and discriminator settings used in this study was 0.52 ± 0.02 . More details will be given in a forthcoming publication [16]. The flux was measured every few hours during exposures. Ion doses were calculated from measured fluxes, exposure times, and the detection efficiency of the MCP. Slow highly charge ion beams from EBIT were stable over long periods, and dose uncertainties due to flux instabilities were typically $<10\%$. Doses of 2×10^{10} (Th^{70+}) and 3×10^{11} (Xe^{27+}) were accumulated over several days. Coverages of $\sim 10^{11}$ – 10^{12} Ga and As atoms per cm^2 on catchers were determined quantitatively by heavy ion backscattering (HIBS) at Sandia National Laboratory [17]. The mass resolution of HIBS did not allow for quantification of the stoichiometry of ablated material. Ablation rates were calculated from surface coverages of Ga and As on the catchers, the ion dose, view factor [14], and the sticking probability of Ga and As atoms on the catcher surface. Secondary ion yields were measured by TOF-SIMS [3].

Total ablation rates are shown in Fig. 1 as a function of projectile charge state q . Projectiles were Xe^{27+} , Xe^{44+} , Th^{56+} , and Th^{70+} with impact velocities of 6.6×10^5 m/s. The relative errors shown in total yield data are dominated by uncertainties in the HIBS results obtained at low surface coverages. Absolute uncertainties, including uncertainties in sticking probabilities and the view factor, are estimated to be $\pm 75\%$. The data at $q = 1+$ give estimates of collisional sputter yields of GaAs for singly charged xenon and thorium projectiles with velocities of 6.6×10^5 m/s as calculated by the TRIM

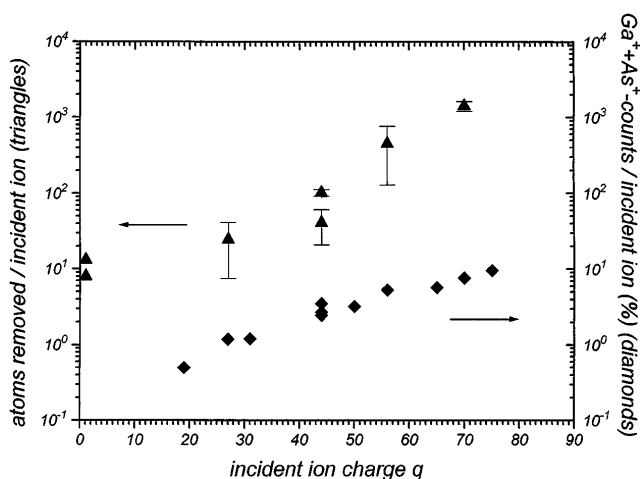


FIG. 1. Total sputtering yields (triangles) and positive secondary ion yields (diamonds) from GaAs(100) as a function of projectile charge state q .

code [18]. The sputtering yield increases from the value for collisional sputtering of ~ 12 atoms/ Th^{1+} to 1410 ± 210 atoms/ Th^{70+} . This total yield is, to our knowledge, the highest sputtering yield observed so far for any bulk semiconductor.

Figure 1 also shows the dependency of secondary ion yields on q . The reported values are the number of positive secondary ions detected per incident ion. Projectiles were Xe^{19+} ($v = 3.9 \times 10^5$ m/s), Xe^{27+} ($v = 6.4 \times 10^5$ m/s), Xe^{44+} ($v = 6.1 \times 10^5$ m/s), Xe^{50+} ($v = 6.6 \times 10^5$ m/s), Th^{56+} ($v = 6.1 \times 10^5$ m/s), Th^{65+} ($v = 5.7 \times 10^5$ m/s), Th^{70+} ($v = 5.9 \times 10^5$ m/s), and Th^{75+} ($v = 6.1 \times 10^5$ m/s). The detection efficiency of the time-of-flight spectrometer with an annular microchannel plate detector η of ~ 0.1 – 0.15 is not included. The error in secondary ion yields is typically $<10\%$. Spectra were dominated by Ga^+ ions and small amounts of As^+ [19]. Positive secondary ion yields increase as a function of q , but the increase is much weaker than for total yields. The number of secondary ions detected per projectile is orders of magnitude smaller than previously observed for oxide targets [3,9]. No significant amounts of secondary cluster ions were detected from GaAs, contrary to results from SiO_2 [3,20] and UO_2 [9]. Positive secondary ion yields exhibited no prominent dependency on the kinetic energy of projectiles. Yields varied by less than 6% when changing the kinetic energy of Th^{70+} ions between 196 keV ($v = 3.9 \times 10^5$ m/s) and 525 keV ($v = 6.6 \times 10^5$ m/s).

The ionization probability α for positive secondary ions is shown in Fig. 2 as a function of q . α is defined here as the number of positive secondary ions emitted per sputtered target atom. α is normalized to the detection efficiency of the TOF-SIMS spectrometer η . The data point for $q = 1+$ gives an estimate of α using the ion yield for Xe^{18+} and the calculated sputtering yield for Xe^{1+} . In striking difference to results for electronic sputtering of

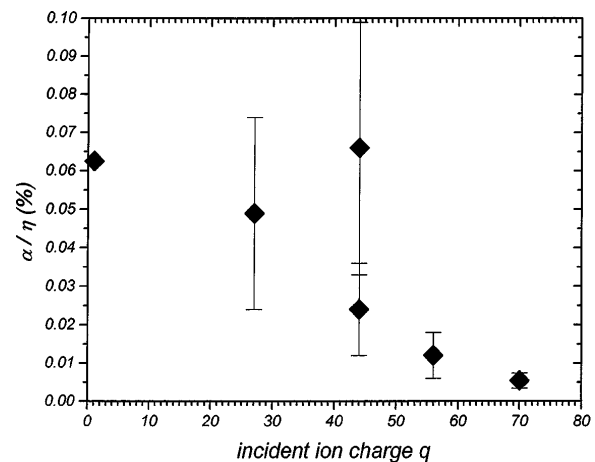


FIG. 2. Ionization probability α for positive secondary ions as a function of projectile charge state q from GaAs(100). The detection efficiency η of the TOF-SIMS spectrometer is ~ 0.1 – 0.15 .

uranium oxide, α is found to decrease with increasing q . For Th^{70+} , α is 2 orders of magnitude smaller than in the electronic sputtering of UO_2 [9].

A model of sputtering induced by SHCI has to describe mechanisms for the conversion of some fraction of the projectiles potential energy (i.e., the sum of the binding energies of electrons removed for the formation of the ion) into kinetic energy of ablated material. One such model is the defect-mediated sputtering model [5]. Localized defects [self-trapped excitons (STE)] are formed in response to valence band excitations in some special materials such as alkali halides and SiO_2 . Sputtering of mostly neutral atoms follows the diffusion of defects to the surface. The absence of a charge state dependent increase of sputtering yields in materials where no STE are known to be formed, such as GaAs(100) [13,21] and MgO, was used as strong evidence for the validity of this model. Our results show that defect-mediated sputtering is not the only mechanism of electronic sputtering by SHCI. The defect model applies only for electronic sputtering of some special materials, and we suspect it applies only under conditions of relatively low excitation densities where the materials response is dominated by the decay of individual defects.

A complementary sputtering model is the Coulomb explosion model [11]. Electron emission in the course of the relaxation of SHCI is thought to form a highly ionized charge domain in insulators and poor conductors. If charge neutrality cannot be reestablished by target electrons on the time scale of lattice vibrations, ~ 0.5 – 1 ps, then electrostatic repulsion of ionized target atoms will force the rapid expansions of material in the charge domain. The emitted material will consist of ions and neutrals. A fraction of the initially ionized material will be reneutralized by target electrons before emission into the vacuum. Total sputtering yields are expected to increase with the charge or the potential energy of projectiles. Also, the fraction of positive secondary ions is predicted to increase with q [11,22–24]. The rapid target expansion in a Coulomb explosion is predicted to cause the formation of a shock wave [22,24]. Large clusters, charged and neutral, are emitted from areas of lower electronic excitation density when the shock wave intersects the target surface. An increase of both total sputtering yields and the ionization probability with q , as well as high yields of positive secondary ions and charged clusters, are observations consistent with this Coulomb explosion model for the interaction of SHCI with oxides such as UO_2 and SiO_2 [3,9,20]. For GaAs, however, the ionization probability decreases with q , and yields of charged clusters are $< 10^{-3}$ counts per Th^{70+} , showing no evidence for the presence of shock waves. Recent model calculations [22] have yielded significant progress over early phenomenological approaches to Coulomb explosion effects. Ionization probabilities for positive secondary ions from silicon targets are calculated to be $\sim (10$ – $17)\%$ [22], very similar to values found for heavy metal oxides interacting with SHCI [9], but much higher than values for GaAs. Important effects such as electronic excitations and charge

transfer processes have so far been neglected. The defect-mediated sputtering model does not apply for GaAs, and presently available Coulomb explosion models [11,22,23] do not reproduce characteristic aspects of semiconductor ablation in the interaction with SHCI.

A third model specifically considers the effect of high density electronic excitations on the structural stability of covalent solids [12]. Evidence for structural instabilities induced by femtosecond laser pulses was recently presented for GaAs(100) [25]. Structural instabilities are nonthermal and arise directly from destabilization of atomic bonds by high density electronic excitations. Non-thermal structural changes are induced in covalent solids when $\sim 10\%$ of valence electrons are promoted from bonding states in the valence band to antibonding states in the conduction band. Each electron-hole excitation causes a repulsive force between atoms. In GaAs, the resulting pressure is predicted to displace atoms by ~ 0.1 nm within only ~ 200 fs [12]. In contrast, heat exchange to the lattice requires many ps. A critical laser fluence to induce such a phase transition in GaAs is ~ 0.8 kJ/m² [12,25] or ~ 5 keV/nm², where a characteristic absorption depth is ~ 1 μm [26]. Potential energies of SHCI used in this study range from 10.5 keV (Xe^{27+}), 51.3 keV (Xe^{44+}), and 67.8 keV (Th^{56+}) to 152.6 keV (Th^{70+}). When these energies are deposited into the volumes discussed below, the energy densities span and considerably exceed this critical value. Recent molecular dynamics simulations of ultrashort pulse laser ablation of silicon have included effects of high density electronic excitations [26]. Ablation rates per laser shot in a high fluence (~ 120 kJ/m²), high energy density (~ 0.75 keV/nm³) regime are ~ 400 – 1000 , the same magnitude as observed for SHCI, such as Th^{56+} and Th^{70+} , interacting with GaAs. Clearly, more detailed simulations on ablation rates, secondary ion yields, and the mass distribution of ablated particles as a function of excitation conditions are highly desirable both for SHCI and femtosecond laser-based excitations.

The first relaxation step in the interaction of SHCI with solids is the formation of a hollow atom above the surface [1,2]. Upon penetration of the solid, target electrons rapidly form a screening cloud around the highly excited projectile. Relaxation proceeds through Auger and radiative transitions. So far only $\sim 10\%$ of the available potential energy of very highly charge ions has been traced in low energy secondary electrons [1,3], x rays [1,27], secondary ions [1,3], and neutrals [5,9]. Screening of a Th^{70+} ion in GaAs induces multiple ionization of target atoms and polarization of the surrounding material. It is plausible to assume that a large ($\gg q$) number of electrons are excited from target atoms surrounding the screened projectile as a result of the massive polarization of the medium and due to electron-electron interaction at very high excitation densities ($> 10^{22}$ cm⁻³) [12]. The zinc blende structure becomes unstable when ~ 1 valence electron per GaAs molecule has been excited into an antibonding state. Relaxation times for ions such as Th^{65+}

or Au⁶⁹⁺ inside solids have been estimated to be only ~ 5 fs [8]. At a velocity of 6.6×10^5 m/s, these ions move ~ 3 nm into the target during relaxation. With this characteristic length we estimate the size of a half sphere effected by primary excitation to be ~ 60 nm³. Relaxation times and, consequently, the excited volume are a function of the projectile charge state. A small fraction of the available energy will be deposited in a much larger volume by energetic Auger electrons and x rays [1,27]. The estimated energy density in a target volume excited by Th⁷⁰⁺ ions is ~ 2 keV/nm³. The expansion driven by electronic excitation is assumed to be isotropic. Atoms thermalize in atomic collisions, and a flux of atoms with net momentum directed towards the surface will contribute to sputtering. The sputtering yield for Th⁷⁰⁺ corresponds to a volume of GaAs under equilibrium conditions of ~ 16 nm³, a fraction of the excited volume. Low secondary ion yields suggest that most of the initially ionized target atoms are reneutralized before they can leave the target. The charge dependent decrease of the ionization probability indicates that the target volume affected by the lattice instability increases faster with q than the ionization density in the excited volume. The efficiency of reneutralization may also increase when atoms are emitted from greater depths. It is not clear why no signatures of shock waves (i.e., charged clusters) are observed as for the rapid expansion associated with Coulomb explosions [3,9,20]. Slow highly charged ions provide a unique way to deposit large amounts of electronic excitation into small volumes of material. Massive sputtering induced by SHCI could lead to novel schemes for the structuring of semiconductor materials on a nanometer scale.

In summary, we have measured sputtering yields and secondary ion yields from GaAs(100) interacting with slow, very highly charge ions. Sputtering yields increase strongly as a function of projectile charge and reach a value of 1410 ± 210 atoms removed per Th⁷⁰⁺ ion. Only a few positive secondary ions are emitted (~ 0.08 counts/Th⁷⁰⁺), and ionization probabilities are an order of magnitude lower than previously determined for oxides. We discuss the application of an ablation model of semiconductors based on structural instabilities induced by intense, ultrafast electronic excitations.

This work was performed under the auspices of the U.S. Department of Energy by Lawrence Livermore National Laboratory under Contract No. W-7405-ENG-48.

-
- [1] D.H. Schneider and M.A. Briere, Phys. Scr. **53**, 228 (1996).
 [2] A. Arnau *et al.*, Surf. Sci. Rep. **229**, 1 (1997).
 [3] T. Schenkel *et al.*, Nucl. Instrum. Methods Phys. Res., Sect. B **125**, 153 (1997); T. Schenkel *et al.*, Mater. Sci. Forum **248-249**, 413 (1997).

- [4] D. Schneider *et al.*, Surf. Sci. **294**, 403 (1993); D.C. Parks *et al.*, Nucl. Instrum. Methods Phys. Res., Sect. B **134**, 46 (1998).
 [5] M. Sporn *et al.*, Phys. Rev. Lett. **79**, 945 (1997); P. Varga *et al.*, Phys. Scr. **T73**, 307 (1997).
 [6] K. Suzuki and N. Itabashi, Pure Appl. Chem. **68**, 1011 (1996).
 [7] K. Mochiji *et al.*, Surf. Sci. **357-358**, 673 (1996); N. Itabashi *et al.*, Jpn. J. Appl. Phys. **34**, 6861 (1995).
 [8] T. Schenkel, M.A. Briere, A.V. Barnes, A.V. Hamza, K. Bethge, H. Schmidt-Böcking, and D. Schneider, Phys. Rev. Lett. **79**, 2030 (1997); T. Schenkel *et al.*, Phys. Rev. Lett. **78**, 2481 (1997).
 [9] T. Schenkel, A.V. Barnes, A.V. Hamza, J.C. Banks, B.L. Doyle, and D.H. Schneider, Phys. Rev. Lett. **80**, 4325 (1998).
 [10] S.T. de Zwart, T. Fried, D.O. Boerma, R. Hoekstra, A.G. Drentje, and A.L. Boers, Surf. Sci. **177**, L939 (1986).
 [11] I.S. Bitensky and E.S. Parilis, J. Phys. C **50**, 227 (1989); I.S. Bitensky, E. Parilis, S. Della-Negra, and Y. Le Beyec, Nucl. Instrum. Methods Phys. Res., Sect. B **72**, 380 (1992).
 [12] P. Stampfli, Nucl. Instrum. Methods Phys. Res., Sect. B **107**, 138 (1996); P. Stampfli and K.H. Bennemann, Appl. Phys. A **60**, 191 (1996).
 [13] N. Itoh, Nucl. Instrum. Methods Phys. Res., Sect. B **122**, 405 (1997).
 [14] D.L. Weathers, T.A. Tombrello, M.H. Prior, R.G. Stokstad, and R.E. Tribble, Nucl. Instrum. Methods Phys. Res., Sect. B **42**, 307 (1989); A. Schnieders, R. Möllers, M. Terhorst, H.-G. Cramer, E. Niehuis, and A. Benninghoven, J. Vac. Sci. Technol. B **14**, 2712 (1996).
 [15] N.R. Daly, Rev. Sci. Instrum. **31**, 264 (1960).
 [16] T. Schenkel *et al.* (to be published).
 [17] J.A. Knapp, D.K. Brice, and J.C. Banks, Nucl. Instrum. Methods Phys. Res., Sect. B **108**, 324 (1996).
 [18] J.P. Biersack, Nucl. Instrum. Methods Phys. Res., Sect. B **27**, 21 (1987).
 [19] R. Matthäus, R. Moshhammer, G.v. Hayn, K. Wien, S. Della-Negra, and Y. Le Beyec, Int. J. Mass Spectrosc. Ion Proc. **126**, 45 (1993).
 [20] T. Schenkel, A.V. Barnes, A.V. Hamza, and D. Schneider, Eur. Phys. J. D **1**, 297 (1998); T. Schenkel, Ph.D. thesis, Johann Wolfgang Goethe Universität, 1997.
 [21] O. Pankratov and M. Scheffler, Phys. Rev. Lett. **75**, 701 (1995).
 [22] H.P. Cheng and J.D. Gillaspay, Phys. Rev. B **55**, 2628 (1997); H.P. Cheng and J.D. Gillaspay, Comput. Mater. Sci. **9**, 285 (1998).
 [23] Y. Yamamura, S.T. Nakagawa, and H. Tawara, Nucl. Instrum. Methods Phys. Res., Sect. B **98**, 400 (1995).
 [24] I.S. Bitensky and E.S. Parilis, Nucl. Instrum. Methods Phys. Res., Sect. B **21**, 26 (1987).
 [25] L. Huang, J.P. Callan, E.N. Glezer, and E. Mazur, Phys. Rev. Lett. **80**, 185 (1998).
 [26] R.F.W. Herrmann, J. Gerlach, and E.E.B. Campbell, Appl. Phys. A **66**, 35 (1998).
 [27] R.E. Marrs, D.H. Schneider, and J.W. McDonald, Rev. Sci. Instrum. **69**, 204 (1998).